



Cite this: *New J. Chem.*, 2016, 40, 6666

# Monitoring thermo-reversible dehydration of the pluronic microenvironment using 4-chloro-1-naphthol as an ESPT fluorescent molecular probe†

Ivy Sarkar

Pluronics are polymeric surfactants that undergo sol–gel phase transition as a function of both temperature and concentration and have a high impact on therapeutics. An excited state proton transfer (ESPT) fluorescent molecular probe, 4-chloro-1-naphthol, has been employed to explore the sol–gel transition of pluronics in aqueous media. In aqueous homogeneous media, 4-chloro-1-naphthol shows anionic emission, whereas in heterogeneous media, it results in dual emission of its neutral and anionic forms. Moreover, variations in the intensity ( $I$ ) ratio,  $I_{\text{neutral}}/I_{\text{anion}}$ , and area ( $A$ ) ratio under the two individual curves,  $A_{\text{neutral}}/A_{\text{anion}}$ , faithfully reflect the progressive changes in the medium heterogeneity. The values of both  $I_{\text{neutral}}/I_{\text{anion}}$  and  $A_{\text{neutral}}/A_{\text{anion}}$  increase with increasing temperature during sol–gel phase transition and reach maxima at the phase transition temperature. Moreover, the higher values of  $I_{\text{neutral}}/I_{\text{anion}}$  and  $A_{\text{neutral}}/A_{\text{anion}}$  in 10% P123 compared to those in F127 signify a lower micro-polarity of the P123 medium compared to that of F127. Evidence of progressive dehydration is obtained from the excited state decay dynamics. It shows that the proton transfer rate decreases remarkably up to the sol–gel transition temperature and after that it remains almost constant. In the present study, thermo-reversible sol–gel transition of pluronics (P123, F127) along with the dehydration of micelles has been monitored with 4-chloro-1-naphthol.

Received (in Montpellier, France)  
27th November 2015,  
Accepted 17th May 2016

DOI: 10.1039/c5nj03354c

www.rsc.org/njc

## Introduction

Molecules having a higher acidity in the excited state are called excited state acids or photoacids<sup>1–5</sup> e.g. naphthols, benzophenones, coumarins, curcumin, falvones, etc.<sup>6–12</sup> Re-distribution of

charge density in the excited state causes facile removal of protons upon photo-excitation.<sup>1–12</sup> Naphthol based excited state proton transfer (ESPT) fluorescent molecular probes are very useful because of their faster proton transfer rates than fluorescence.<sup>13</sup> For example, 1-naphthol ( $pK_a = 9.2$ ,  $pK_a^* = 0.4$ ) is a well-known ESPT fluorescent molecular probe that has been used frequently in biological and physical studies.<sup>13–21</sup> With a large difference between the  $pK_a$  (8.75) and  $pK_a^*$  (1.73) values, 4-chloro-1-naphthol, a 1-naphthol derivative, can also be used as an effective ESPT fluorescent molecular probe.<sup>22</sup> Here, the electron withdrawing inductive effect of chlorine helps in stabilizing the conjugate base of 4-chloro-1-naphthol in the excited state.<sup>22</sup> As described by Pappayee *et al.*, 4-chloro-1-naphthol is a potential but rarely used ESPT molecular probe among the naphthol derivatives.<sup>22</sup> Fig. 1 shows the molecular structure of 4-chloro-1-naphthol and a schematic representation of its ESPT process. 4-Chloro-1-naphthol is mainly used as a staining agent. In the presence of peroxide, horseradish peroxidase (HRP) catalyzes the oxidation of 4-chloro-1-naphthol to 4-chloro-1-naphthone. This allows easy chromogenic detection which can be photographed easily.<sup>23–28</sup> But unlike those on 1-naphthol, there are very few photo-physical studies that describe the potential of 4-chloro-1-naphthol as a probe of organized media.<sup>22,29–31</sup>

Department of Chemistry, Indian Institute of Technology Madras, Chennai – 600 036, India. E-mail: ivysarkar111@gmail.com

† Electronic supplementary information (ESI) available: Fluorescence spectra of 4-Cl-1-naphthol in water with temperature, variation in the fluorescence intensity of the neutral and anionic forms of 4-Cl-1-naphthol in 10% P123 and 10% F127 media with increasing temperature, intrinsic fluorescence of 10% P123 and 10% F127, subtracted fluorescence spectra of 4-Cl-1-naphthol in (a) 10% P123 and (b) 10% F127 media as a function of temperature, at  $\lambda_{\text{ex}}$  290 nm, double Gaussian fitting of the subtracted spectra of 4-Cl-1-naphthol in 10% P123 media with temperature, double Gaussian fitting of the subtracted spectra of 4-Cl-1-naphthol in 10% F127 media with temperature, the area under the two curves in 10% P123 media, (a) neutral and (b) anionic forms, and 10% F127 media, (c) neutral and (d) anionic forms. Residue distribution plots of 4-Cl-1-naphthol in water at different temperatures, residue distribution plots of the neutral form of 4-Cl-1-naphthol in 10% P123 media at different temperatures, residue distribution plots of the neutral form of 4-Cl-1-naphthol in 10% F127 media at different temperatures, residue distribution plots of the anionic form of 4-Cl-1-naphthol in 10% P123 media at different temperatures, residue distribution plots of the anionic form of 4-Cl-1-naphthol in 10% F127 media at different temperatures, and intrinsic fluorescence lifetime data of pluronics at 20 °C ( $\lambda_{\text{ex}} = 295$  nm and  $\lambda_{\text{em}} = 460$  nm). See DOI: 10.1039/c5nj03354c

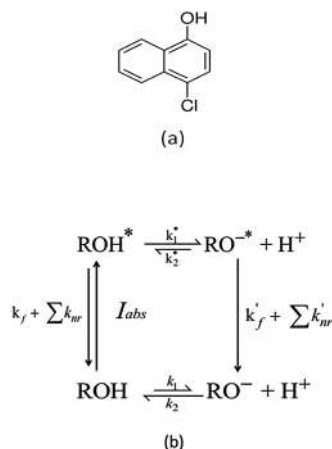


Fig. 1 (a) Molecular structure of 4-chloro-1-naphthol and (b) a schematic representation of the ESPT process.

In water, 4-chloro-1-naphthol remains in the ground state neutral form, which upon photo-excitation undergoes the ESPT process to form anion. Four water molecules make a cluster, which acts as a base to solvate the proton ejected by the photo-acid.<sup>32</sup> As a result, in aqueous medium, emission arises from the anionic (470 nm) form entirely. With a decrease in the polarity and availability of water, this anionic peak diminishes along with an increase in the neutral peak (360 nm).<sup>16,22</sup> Because of having two distinct emitting states, it acts as a multi-domain probe in micro-heterogeneous media.<sup>22</sup> The prototropic equilibrium between the anionic and neutral forms is highly sensitive to micro-environmental changes, which is evident from the alteration in the emission intensity ratio.<sup>22</sup> A fascinating aspect of this ESPT molecule has been employed here to follow the thermotropic micro-environmental changes in pluronic co-polymers P123 and F127.

Pluronics are water soluble tri-block copolymers (PEO<sub>x</sub>-PPO<sub>y</sub>-PEO<sub>x</sub>, *x* and *y* vary for different varieties of pluronics) composed of hydrophilic poly(ethyleneoxide) (PEO) and hydrophobic poly(propylene oxide) (PPO) units.<sup>33</sup> These polymers possess amphiphilicity due to the temperature induced preferential solubility of one unit over another.<sup>34,35</sup> As a result, they form spherical micelles and gels, as a function of both temperature and concentration.<sup>36,37</sup> The highly hydrophobic anhydrous inner core region of these micelles helps in solubilizing water insoluble drug molecules.<sup>37-39</sup> A highly swollen hydrophilic outer surface, the corona, aids the water solubility of these polymers.<sup>40-43</sup> Here, two pluronic varieties, hydrophobic P123 (PEO<sub>20</sub>-PPO<sub>70</sub>-PEO<sub>20</sub>) and hydrophilic F127 (PEO<sub>100</sub>-PPO<sub>64</sub>-PEO<sub>100</sub>), have been used to monitor the temperature induced changes. 10% solutions of pluronics have been used over a range of temperatures, such that the solutions remain above the CMC (Critical Micellar Concentration) or CMT (Critical Micellar Temperature) but below the transparent hydrogel.<sup>37,44,45</sup> It is known that monomeric units of pluronics are responsible for their biological activities.<sup>40</sup> Hence, in drug compositions, these polymers are used at higher concentrations, so that they dissociate into monomers in the blood stream.<sup>40</sup> In our

previous work, an aggregate forming coumarin-cholesterol conjugate (Cum-Chl) was used to investigate the micro-polarity difference and sol-gel transition of pluronics.<sup>41</sup> A characteristic fluorescence feature of Cum-Chl,  $I_{\text{monomer}}/I_{\text{aggregate}}$ , was used for that purpose. Here, a conceptually different, easily usable, commercially available, ESPT fluorescent molecular probe has been employed in pluronic media to assess its progressive dehydration during sol-gel transition with the aid of its  $I_{\text{neutral}}/I_{\text{anion}}$  and  $A_{\text{neutral}}/A_{\text{anion}}$  values, the shift in its emission maxima and the lifetime of two prototropic forms. The use of such small fluorescent molecular probes is sometimes beneficial because of their minimum perturbation into the investigating system as compared to that by aggregate forming bulky molecular probes.<sup>41</sup> Moreover, systems can be monitored at two different wavelengths, with ESPT probes having largely separated emission spectra. Also, the fluorescence lifetimes of the ESPT probe help us to calculate the proton transfer rate, which is an indicator of progressive dehydration.

The specific objectives of this paper are (i) to follow the sol-gel phase transition, (ii) to monitor the sensitivity of 4-chloro-1-naphthol towards the micro-polarity of different pluronics using  $I_{\text{neutral}}/I_{\text{anion}}$  and  $A_{\text{neutral}}/A_{\text{anion}}$  values and (iii) to probe the dehydration and modulation of the ESPT process with sol-gel transition using fluorescence lifetime data.

## Experimental

### Materials

Pluronic P123, F127 and 4-chloro-1-naphthol were purchased from Sigma Chemical Co. (Bangalore, India). Sodium di-hydrogen phosphate and di-sodium hydrogen phosphate were purchased from Merck Specialties Pvt. Ltd (Mumbai, India). The same batch of pluronics has been used for all experiments. The triple distilled water used in all experiments was prepared using KMnO<sub>4</sub> and NaOH. Spectroscopic grade ethanol was used for preparing the stock solution of the probe.

### Preparation of pluronic solutions

10% (w/v) solutions of pluronic P123 and F127 in pH 7 phosphate buffer were used for the temperature dependent experiments. The temperature was varied from 5–24 °C and 13–34 °C, respectively, for P123 and F127 solutions. As pluronics are soluble only in cold water, the polymeric solutions were kept in a fridge to ensure complete dissolution. Then, aqueous probe solution was added to the prepared polymeric solutions and kept over-night to ensure homogeneity.

### Steady state and time resolved fluorescence measurements

Steady state fluorescence measurements were performed using the Fluoromax 4 (Horiba Jobin Yvon) spectrofluorimeter with a 150 W Xenon lamp as a source of excitation. A 3/3 slit width has been used for all experiments. Data were acquired for the lifetime experiments using the Horiba Jobin Yvon TCSPC lifetime instrument in a time-correlated single-photon counting arrangement. A nano-LED of 295 nm was used as the excitation source.

The pulse repetition rate was set at 1 MHz. The instrumental full width at half-maxima of the 295 nm LED, including the detector response, was measured to be  $\sim 800$  ps. The instrument response function was obtained using scattered medium, LUDOX AS40 colloidal silica. IBH software was used for decay analysis. Decays were fitted to obtain a symmetric distribution, keeping the  $\chi^2$  value in the range  $0.99 \leq \chi^2 \leq 1.4$ . The average fluorescence lifetime ( $\tau_{\text{aveg}}$ ) was calculated using the following equation, where  $\tau_i$  is the lifetime of a component with amplitude  $\beta_i$  and  $i$  signifies the number of components present.<sup>46</sup>

$$\tau_{\text{average}} = \frac{\sum_{i=1}^n \beta_i \tau_i}{\sum_{i=1}^n \beta_i}$$

An ethanolic solution of 4-chloro-1-naphthol was used as the stock solution for all experiments and was finally diluted with water. Ethanol contamination was kept to less than 1% to avoid any kind of interference. The final probe concentration was maintained at 2.5  $\mu\text{M}$  for all experiments. The desired temperature was controlled by water circulation through the jacketed cuvette holder from a refrigerated bath (Julabo, Germany).

## Results and discussion

### Steady state fluorescence spectroscopy data

Here, the steady state fluorescence response of 4-Cl-1-naphthol has been monitored during sol-gel transition of pluronics. It was found that 10% P123 and 10% F127 undergo sol-gel transition at 15 °C and 21 °C, respectively.<sup>41</sup> In aqueous medium, the emission of 4-Cl-1-naphthol only originates from anionic species ( $\text{RO}^-*$ ), ESI,† Fig. S1. This anionic emission decreases slightly with increasing temperature. However, in the presence of polymeric heterogeneity, both anionic ( $\text{RO}^-*$ ) and neutral forms ( $\text{ROH}^*$ ) of emission are observed.<sup>16,17,21,22</sup> Fig. 2a and b show the fluorescence spectra of 4-Cl-1-naphthol as a function of temperature in the presence of 10% P123 and 10% F127, respectively. The intensity of the neutral form has been found to increase along with a concomitant decrease in the anionic emission intensity with increasing temperature. An iso-emissive region at  $\sim 415$  nm signifies two state equilibrium between the neutral and anionic forms. This indicates that the ratio of the intensities of the neutral and anionic forms,  $I_{\text{neutral}}/I_{\text{anion}}$ , can be a reliable tool to monitor thermo-reversible sol-gel transition.

$I_{\text{neutral}}/I_{\text{anion}}$  values calculated from Fig. 2 along with the blue shift in the anionic emission have been used to monitor the change in the pluronic micro-environment. Fig. 3a and c show the variation of  $I_{\text{neutral}}/I_{\text{anion}}$  values as a function of temperature in P123 and F127 media, respectively. With increasing temperature,  $I_{\text{neutral}}/I_{\text{anion}}$  increases significantly up to the sol-gel transition temperature (Fig. 3a and c) and after that it decreases slightly. Individual emission intensities of both the neutral and anionic forms also follow the sol-gel transition. Both the increase in the neutral emission intensity (ESI,† Fig. S2a for 10% P123 and Fig. S2c for 10% F127) and the decrease in the anionic emission intensity (ESI,† Fig. S2b for 10% P123 and Fig. S2d for 10% F127)

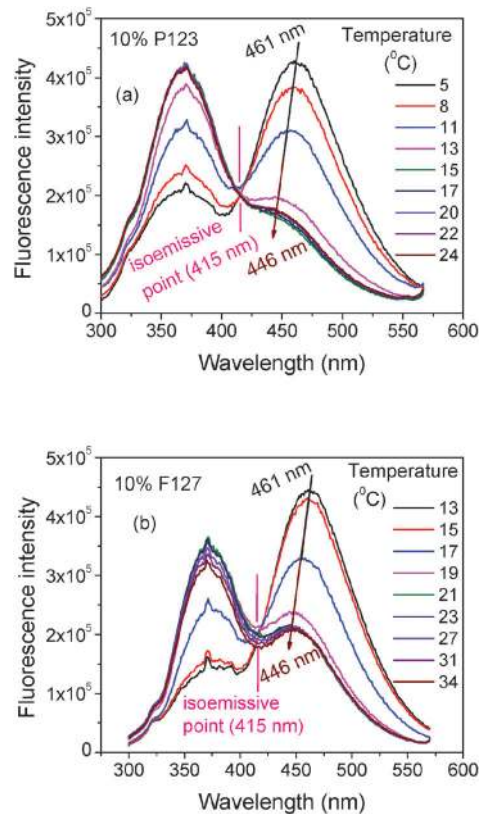


Fig. 2 Fluorescence spectra of 4-Cl-1-naphthol in (a) 10% P123 and (b) 10% F127 media as a function of temperature;  $\lambda_{\text{ex}}$  290 nm.

show onset at the sol-gel transition temperature. In polymeric sol media, anionic emission (461 nm) is blue shifted as compared to that in aqueous media (470 nm) due to the increased non-polarity in the presence of pluronics (Fig. 3b and d). Moreover, the anionic emission maxima have been found to undergo a hypsochromic shift of  $\sim 15$  nm (from 461 nm in the sol phase to 446 nm in the gel phase) with sol-gel transition (Fig. 3b and d). The blue shift of the anionic emission maxima follows the sol-gel transition of the respective pluronics (Fig. 3b and d). A shift in the anionic emission maxima has also been found with 1-naphthol in the F127 medium.<sup>21</sup> In the sol state, pluronics are known to be in the spherical micellar form, which is highly hydrated in solution. The corona region of PEO units is known to swell to twice its actual volume in the presence of water.<sup>47</sup> As the temperature increases, the hydrogen bonds of PEO units with water molecules break down, leading to an increase in hydrophobic interaction. This enhanced hydrophobic interaction induces hydrogel formation, which shrinks the corona region in its cubic gel phase.<sup>48</sup> As a result, hypsochromic shift of the emission maxima and intensity variations of both the neutral and anionic forms have been observed (Fig. 2). This kind of polarity change is more pronounced before sol-gel transition. As a result, all of the fluorescence parameters undergo a considerable change up to the sol-gel transition temperature.<sup>49,50</sup> The slight decrease in the  $I_{\text{neutral}}/I_{\text{anion}}$  value above the sol-gel transition temperature is due to the expulsion of the small molecular probe from the micellar media into

the aqueous bulk.<sup>49</sup> A similar response of steady state fluorescence parameters has also been observed for 1-naphthol in the pluronic F127 medium.<sup>21</sup>

Two different prototropic forms (neutral and anionic) of 4-Cl-1-naphthol report from two different micro-domains of polymeric micelles.<sup>51</sup> Being neutral in nature, ROH\* emission is expected to originate from the core region and core–corona interface of the micelle, whereas, RO<sup>−</sup>\* emission originates mostly from the interfacial region. This has been further discussed in the next section with the help of lifetime data. From Fig. 3a and c it is clear that  $I_{\text{neutral}}/I_{\text{anion}}$  has a higher value in the 10% P123 medium than that in the 10% F127 medium. This is due to the higher hydrophobicity of P123 (HLB index, 8), which favors a more neutral population than that favored by F127 (HLB index, 22).<sup>39</sup> Here,  $I_{\text{neutral}}/I_{\text{anion}}$  not only follows the thermo-reversible sol–gel transition but also reflects the differences in the hydrophobicities of polymeric media. In our previous publication, synthesized probe molecule Cum–Chl was used to study the sol–gel phase transition and micro-polarity of pluronics using its  $I_{\text{monomer}}/I_{\text{aggregate}}$  parameter.<sup>41</sup> The polarity driven partitioning of Cum–Chl H-aggregates in micellar media as their monomers was the key factor to determine the  $I_{\text{monomer}}/I_{\text{aggregate}}$  ratio. Here, in the present investigation, the polarity induced proton transfer of 4-Cl-1-naphthol has been used as the principle of analysis.

In connection to this, it is important to note that both the polymers, P123 and F127, have intrinsic fluorescence, which mostly contaminates the neutral form emission and slightly contaminates the anionic emission, as evident from ESI,† Fig. S3a and b. The contribution of intrinsic fluorescence is negligible as compared to that of the emission of the neutral form of 4-Cl-1-naphthol, as seen in the ESI,† Fig. S3a and b (intrinsic fluorescence has been plotted on the same scale as the probe's emission intensity). Moreover, this intrinsic fluorescence doesn't change with temperature, unlike the neutral form of fluorescence.<sup>21</sup> Additionally, as the intensity of the neutral form increases with temperature the contribution of intrinsic fluorescence becomes progressively insignificant. In Fig. S4 (ESI,†), the intrinsic fluorescence of pluronics (ESI,† Fig. S3) has been subtracted from the spectra of 4-Cl-1-naphthol in pluronic media (Fig. 2) to obtain more reliable spectra. It shows that the newly obtained spectra (ESI,† Fig. S4) do not alter the previous conclusion obtained from Fig. 2. The subtracted spectra have been fitted with the double Gaussian function (ESI,† Fig. S5 and S6) to visualize the individual spectra. From this, the area under the fitted curves has been calculated, which indicates the contribution of two different prototropic forms. Like the intensity ratio ( $I_{\text{neutral}}/I_{\text{anion}}$ ), the area ratio of the two forms ( $A_{\text{neutral}}/A_{\text{anion}}$ ) has been plotted in Fig. 4, which has been found to follow the sol–gel transition of the respective pluronics. The individual areas under the plots also follow the sol–gel transition of 10% P123 and 10% F127 (Fig. S7, ESI,†). The insignificant contributions of the neutral form in the 10% F127 medium at initial temperatures (13 and 15 °C) have been taken as zero as they could not be fitted with the double Gaussian function. A higher value of  $A_{\text{neutral}}/A_{\text{anion}}$  in the 10%

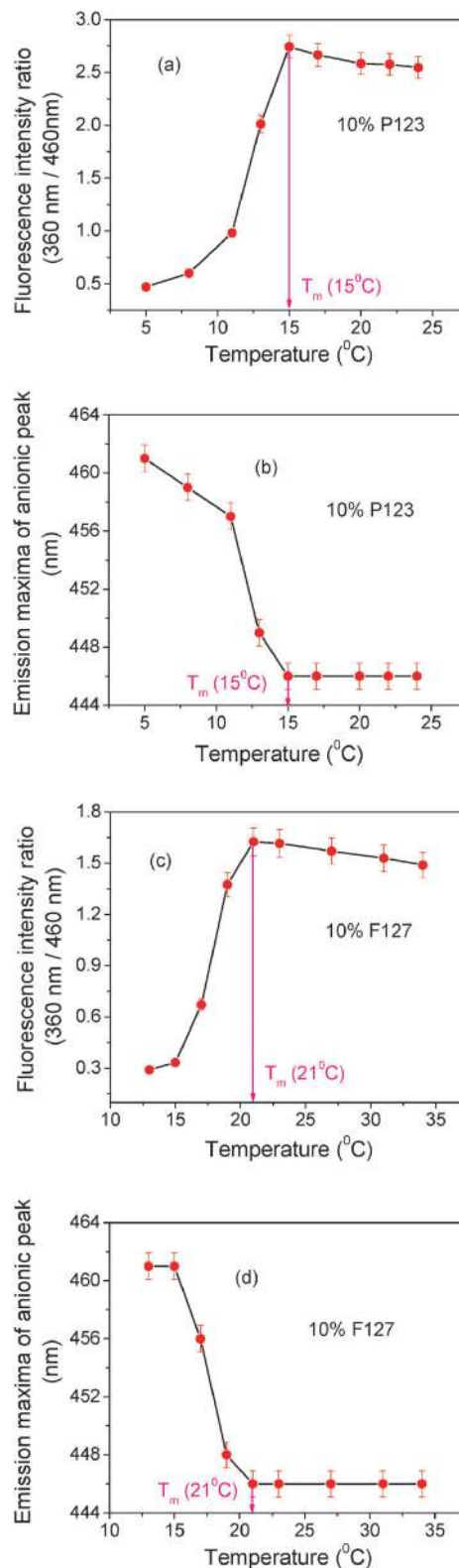


Fig. 3 (a) Variation of  $I_{\text{neutral}}/I_{\text{anion}}$  and (b) anionic emission maxima of 4-Cl-1-naphthol in 10% P123 media as a function of temperature; (c) Variation of  $I_{\text{neutral}}/I_{\text{anion}}$  and (d) anionic emission maxima of 4-Cl-1-naphthol in 10% F127 media as a function of temperature;  $\lambda_{\text{ex}}$  290 nm.

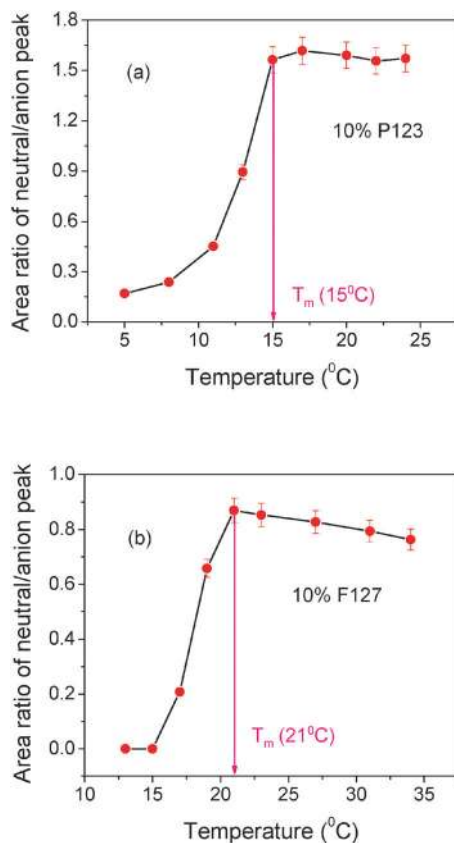


Fig. 4 Variation of  $A_{\text{neutral}}/A_{\text{anion}}$  in 10% (a) P123 and (b) F127 media with temperature;  $\lambda_{\text{ex}} = 290$  nm.

P123 medium compared to that in the 10% F127 medium indicates a higher contribution of the neutral form in the P123 medium. This is due to the lower micro-polarity of P123 micelles than that of F127 micelles.

### Time resolved fluorescence spectroscopy data

The excited state decay dynamics has been analyzed after monitoring the steady state fluorescence parameters of 4-Cl-1-naphthol during sol-gel transition of pluronics. Fig. 5 represents the fluorescence lifetime decay of 4-Cl-1-naphthol in water with temperature. The lifetime of anionic decay ( $\text{RO}^{-*}$ ,  $\lambda_{\text{ex}} = 295$  nm,  $\lambda_{\text{em}} = 470$  nm) has been fitted with a single exponential function, showing a lifetime of  $\sim 9$  ns, matching closely with the literature value.<sup>22</sup> In addition, this lifetime is found to decrease marginally with increasing temperature, which is consistent with the steady state data. The fluorescence lifetime of the 4-Cl-1-naphthol anion in water as a function of temperature has been enlisted in Table 1. Residue distribution plots for the same have been given in the ESI,<sup>†</sup> Fig. S8.

In the presence of pluronic P123 and F127, emissions have been monitored for both the neutral ( $\lambda_{\text{ex}} = 295$  nm,  $\lambda_{\text{em}} = 360$  nm) and anionic ( $\lambda_{\text{ex}} = 295$  nm,  $\lambda_{\text{em}} = 460$  nm) forms. Fig. 6a and b show the fluorescence lifetime decay profiles of the neutral form of emission as a function of temperature in P123 and F127 media, respectively. As expected from the steady state data, the fluorescence lifetime decay of the neutral form is

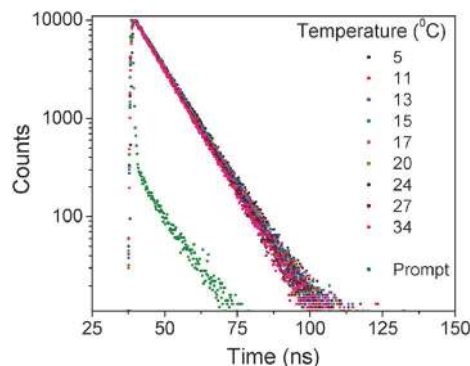


Fig. 5 Fluorescence lifetime decay profiles of the 4-Cl-1-naphthol anion ( $\lambda_{\text{ex}} = 295$  nm,  $\lambda_{\text{em}} = 470$  nm) in water as a function of temperature.

Table 1 Fluorescence lifetime data of the 4-Cl-1-naphthol anion ( $\lambda_{\text{ex}} = 295$  nm,  $\lambda_{\text{em}} = 470$  nm) in water as a function of temperature

Temperature ( $^{\circ}\text{C}$ )	$\tau$ ( $\beta$ )	$\chi^2$
5	9.47 (1)	1.09
11	9.33 (1)	1.05
13	9.30 (1)	1.28
15	9.19 (1)	1.21
17	9.15 (1)	1.24
20	9.11 (1)	1.17
24	9.06 (1)	1.19
27	8.99 (1)	1.26
34	8.83 (1)	1.19

contaminated slightly by the intrinsic fluorescence of the pluronics. But this contamination does not induce any ambiguity in the analysis as it is separable after fitting. Fluorescence decay of the neutral form in pluronic media have been fitted with a triple exponential function. The lifetime data of the neutral form as a function of temperature have been provided in Tables 2 and 3 for P123 and F127 media, respectively. The residue distribution plots for the same have been given in the ESI,<sup>†</sup> Fig. S9 and S10. The longest lifetime component ( $\tau_3$ , 14–25 ns) with least contribution ( $\beta_3$ , 0.01–0.03) originates from the intrinsic fluorescence of the pluronics.<sup>21</sup> Similar to the steady-state data, intrinsic fluorescence has a negligible contribution over lifetimes and it decreases with increasing temperature.<sup>21</sup> The  $\sim 3$ –4 ns lifetime component ( $\tau_2$ ) originates from the anhydrous core region, whereas the shortest lifetime component ( $\tau_1$ ,  $\sim 1$ –2 ns) originates from the corona and core-corona interfacial region of the micelles. In the literature, it has been found that the longer lifetime component of the 1-naphthol neutral form originates from the relatively anhydrous and hydrophobic core region.<sup>17,21</sup> The core region is more rigid as compared to the hydrated corona region, and as a result, non-radiative decay is less in the core.<sup>51</sup> This reflects in the higher value of the fluorescence lifetime in the relatively anhydrous and non-polar core region.<sup>16,17,21</sup> The values of both  $\tau_1$  and  $\tau_2$  increase from the sol state to the gel state and are the highest at the sol-gel transition temperatures of the respective pluronics. As the changes in pluronic micelles are more pronounced up to the sol-gel transition temperature,<sup>41,49,50</sup>

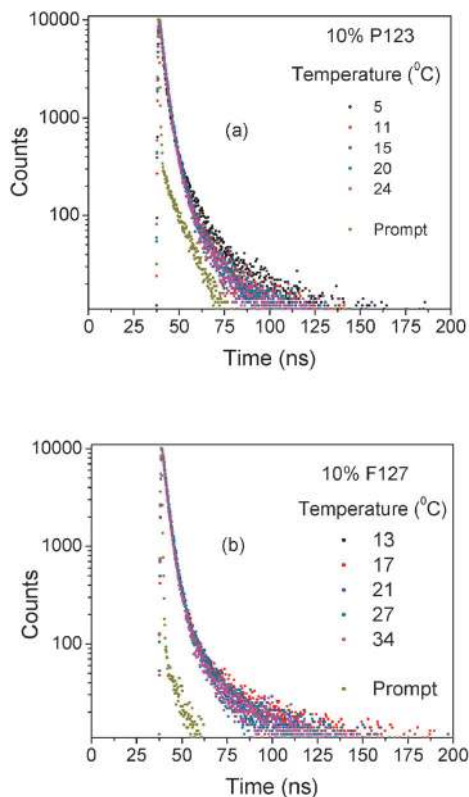


Fig. 6 Fluorescence lifetime decay profiles of the neutral form of 4-Cl-1-naphthol ( $\lambda_{\text{ex}} = 295$  nm,  $\lambda_{\text{em}} = 360$  nm) in (a) 10% P123 and (b) 10% F127 media as a function of temperature.

Table 2 Fluorescence lifetime data of the neutral form of 4-Cl-1-naphthol ( $\lambda_{\text{ex}} = 295$  nm,  $\lambda_{\text{em}} = 360$  nm) in 10% P123 media as a function of temperature

Temperature ( $^{\circ}\text{C}$ )	$\tau_1$ ( $\beta_1$ )	$\tau_2$ ( $\beta_2$ )	$\tau_3$ ( $\beta_3$ )	$\chi^2$
5	1.10 (0.66)	3.48 (0.31)	14.52 (0.03)	1.22
11	1.67 (0.52)	3.57 (0.46)	14.15 (0.02)	1.18
15	2.21 (0.72)	4.72 (0.27)	19.22 (0.01)	1.02
20	2.09 (0.70)	4.27 (0.29)	18.43 (0.01)	1.18
24	2.11 (0.71)	4.10 (0.28)	15.28 (0.01)	1.09

Table 3 Fluorescence lifetime data of the neutral form of 4-Cl-1-naphthol ( $\lambda_{\text{ex}} = 295$  nm,  $\lambda_{\text{em}} = 360$  nm) in 10% F127 media as a function of temperature

Temperature ( $^{\circ}\text{C}$ )	$\tau_1$ ( $\beta_1$ )	$\tau_2$ ( $\beta_2$ )	$\tau_3$ ( $\beta_3$ )	$\chi^2$
13	1.09 (0.53)	3.29 (0.45)	16.38 (0.02)	1.22
17	1.41 (0.60)	3.62 (0.39)	18.07 (0.01)	1.14
21	2.37 (0.79)	4.86 (0.20)	20.20 (0.01)	1.01
27	2.07 (0.72)	4.10 (0.27)	17.66 (0.01)	1.23
34	2.10 (0.82)	4.98 (0.17)	25.47 (0.01)	1.16

$\tau_1$  and  $\tau_2$  show the highest values at the phase transition temperature. After that the lifetime value decreases slightly due to the increase in non-radiative decay with increasing temperature.<sup>41</sup> Bi-exponential decay of the neutral emission, excluding intrinsic pluronic decay, signifies its distribution over different sites of pluronic micelles.<sup>51</sup> Similar lifetime

distributions have also been found earlier for the parent, 1-naphthol, and the neutral form of 4-Cl-1-naphthol in various micro-heterogeneous media.<sup>16,17,21,22</sup> In liposome media, the shorter lifetime ( $\sim 1$  ns) and longer lifetime ( $\sim 4$  ns) components of the neutral form of 4-Cl-1-naphthol had been assigned to the interfacial and interior populations, respectively.<sup>22</sup> Here, a higher  $\beta_1$  compared to  $\beta_2$  indicates a greater population of the probe in the interfacial region.

Fig. 7a and b show the fluorescence lifetime decay profiles of the anionic emission of 4-Cl-1-naphthol as a function of temperature in P123 and F127 media, respectively. In pluronics, anionic decay has been fitted with a double exponential function. The lifetime data of the anionic form as a function of temperature have been given in Tables 4 and 5 for P123 and F127 media, respectively. The residue distribution plots for the same have been given in the ESI,<sup>†</sup> Fig. S11 and S12. It has been found that

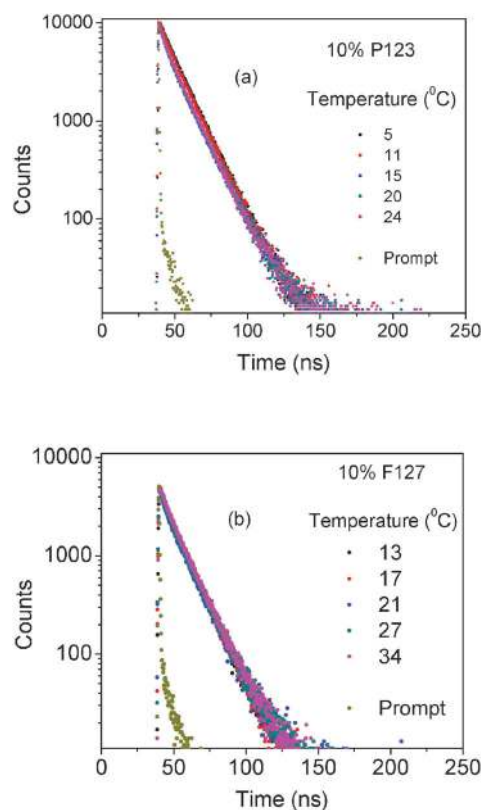


Fig. 7 Fluorescence lifetime decay profiles of the anionic form of 4-Cl-1-naphthol ( $\lambda_{\text{ex}} = 295$  nm,  $\lambda_{\text{em}} = 460$  nm) in (a) 10% P123 and (b) 10% F127 media as a function of temperature.

Table 4 Fluorescence lifetime data of the anionic form of 4-Cl-1-naphthol ( $\lambda_{\text{ex}} = 295$  nm,  $\lambda_{\text{em}} = 460$  nm) in 10% P123 media as a function of temperature

Temperature ( $^{\circ}\text{C}$ )	$\tau_1$ ( $\beta_1$ )	$\tau_2$ ( $\beta_2$ )	$\chi^2$
5	5.58 (0.23)	14.34 (0.77)	1.07
11	5.04 (0.19)	14.34 (0.81)	1.16
15	4.82 (0.34)	14.77 (0.66)	1.07
20	4.39 (0.27)	14.40 (0.73)	1.13
24	4.04 (0.29)	14.15 (0.71)	1.07

**Table 5** Fluorescence lifetime data of the anionic form of 4-Cl-1-naphthol ( $\lambda_{\text{ex}} = 295$  nm,  $\lambda_{\text{em}} = 460$  nm) in 10% F127 media as a function of temperature

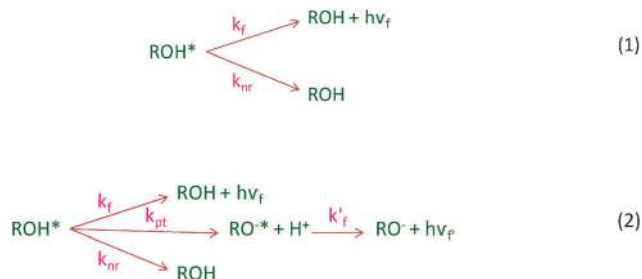
Temperature ( $^{\circ}\text{C}$ )	$\tau_1$ ( $\beta_1$ )	$\tau_2$ ( $\beta_2$ )	$\chi^2$
13	3.88 (0.23)	13.35 (0.77)	1.22
17	3.77 (0.22)	13.42 (0.78)	1.16
21	3.59 (0.34)	13.99 (0.66)	1.29
27	3.89 (0.30)	13.97 (0.70)	1.12
34	4.41 (0.20)	13.81 (0.80)	1.12

the anionic emission is slightly contaminated by the intrinsic fluorescence of the pluronics due to the presence of its tail towards the longer wavelength. The shorter component ( $\tau_1$ , 3–5 ns) originates from the intrinsic fluorescence of the pluronics (ESI,† Table S1), whereas the longer component ( $\tau_2$ , 13–14 ns) originates from the anionic form of 4-Cl-1-naphthol in the presence of pluronics. The anionic lifetime of 4-Cl-1-naphthol in pluronics is higher as compared to that in aqueous media and it does not change with increasing temperature because of its interfacial location. As the probe is bound to the polymer interface, the rate of non-radiative decay decreases, leading to an increase in the fluorescence lifetime.<sup>52</sup> Unlike 1-naphthol, the anionic form of 4-Cl-1-naphthol does not show any distributive nature because of its higher polarity due to the presence of the chloro group. The non-distributive nature of the anionic form of 4-Cl-1-naphthol has also been found earlier in liposome media.<sup>22</sup> In contrast to the anionic form, the neutral form has been found to undergo multi-domain distribution, which can be attributed to the less polar character of the neutral form.<sup>22</sup> For 1-naphthol, the rise time (3–4 ns) of anionic fluorescence implies that in the hydrophobic pluronic environment the ionization rate constant of 1-naphthol was significantly reduced.<sup>21</sup> This has not been observed here with 4-Cl-1-naphthol. This is possibly due to the faster rate of proton transfer from 4-Cl-1-naphthol due to the electron withdrawing stabilizing effect of the chloro group at its *para* position.

In heterogeneous media, the origin of the lifetime components of such ESPT molecular probes can be assigned easily. But this is very complicated for aggregate forming probe molecules.<sup>41</sup> In addition, aggregates cause scattering of light due to their larger sizes, which leads to difficulty in analysis. This is a significant advantage of using small molecular probes for sensing micro-environmental changes in organized media.

### Determination of the ESPT rate

The proton transfer rate of an ESPT molecule is directly related to its degree of hydration.<sup>16,21</sup> The accessibility of water molecules regulates the polarity of heterogeneous media, which manifests as variations in lifetime data. Hence, from the lifetime values of 4-Cl-1-naphthol in different domains, the rate of the ESPT process can be calculated. For this purpose, a simple model has been adopted that assumes that in the dry core region ESPT is completely restricted but it is allowed in the interfacial region.<sup>21</sup> Accordingly, the photo-processes involved after excitation at the core (1) and interfacial region (2) can be expressed as follows (Scheme 1):<sup>21</sup>



**Scheme 1** Photo-processes of 4-Cl-1-naphthol in the (1) core and (2) interfacial region after excitation.

here,  $k_f$ ,  $k'_f$  = rate constant of the radiative process,  $k_{\text{nr}}$  = rate constant of the non-radiative process,  $k_{\text{pt}}$  = rate constant of proton transfer.

The corresponding lifetimes of the two domains can be expressed as follows:

$$\tau_{\text{core}} = 1/(k_f + k_{\text{nr}}) \quad (3)$$

$$\tau_{\text{interface}} = 1/(k_f + k_{\text{nr}} + k_{\text{pt}}) \quad (4)$$

Thus, it is obvious that the proton transfer rate ( $k_{\text{pt}}$ ) can be determined from the difference in two lifetime reciprocals:

$$k_{\text{pt}} = (1/\tau_{\text{interface}}) - (1/\tau_{\text{core}}) \quad (5)$$

Fig. 8a and b show the modulation of the proton transfer rate as a function of temperature in P123 and F127 media, respectively.

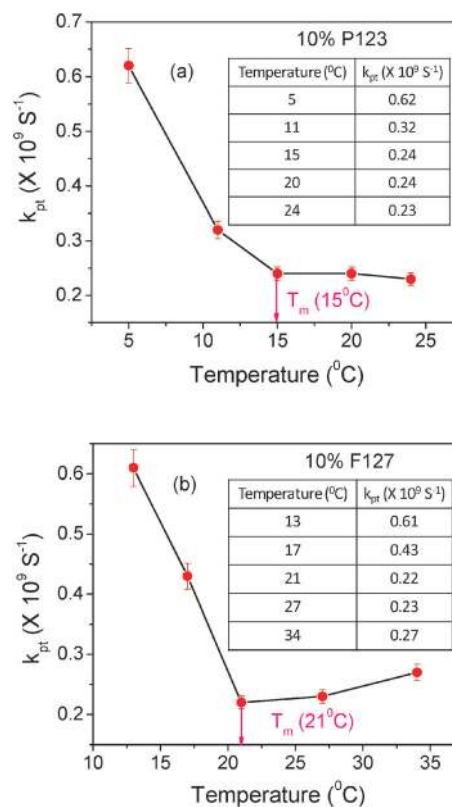


**Fig. 8** Variation of the proton transfer rate in (a) 10% P123 and (b) 10% F127 media with temperature.

There is a sharp decrease in the proton transfer rate with increasing temperature in the sol phase and after sol-gel transition it remains almost constant. This signifies the progressive dehydration of pluronic micelles during sol-gel transition. This kind of dehydration process can be visualized easily with ESPT molecular probes but not with aggregate forming probes.<sup>41</sup> Reports show that 1-naphthol has already been used to monitor the level of hydration of different media (e.g. pluronics, the lipid bilayer membrane in the presence of submicellar bile salts, polyvinyl alcohol (PVA) films, etc.).<sup>16,18,21</sup>

## Conclusions

The sensitivity of excited state proton transfer (ESPT) fluorescent molecular probe 4-chloro-1-naphthol has been assessed to investigate the thermo-reversible sol-gel transition of pluronics. Being present in two different prototropic forms of different polarities, this molecule serves as a multi-domain probe, distributing over various possible micro-domains of pluronics (e.g. core, corona, interface, etc.). The multi-domain distribution of 4-chloro-1-naphthol is advantageous over that of various known fluorophores. Lifetime components with different orders of magnitude also support its distributive nature. The neutral form emission, which arises from the micellar region, increases with increasing temperature. Anionic emission, arising from the interfacial region, decreases with increasing temperature with a blue shift. This makes  $I_{\text{neutral}}/I_{\text{anion}}$  a sensitive parameter for sol-gel transition. The sensitivities of all fluorescence parameters ( $I_{\text{neutral}}/I_{\text{anion}}$ ,  $A_{\text{neutral}}/A_{\text{anion}}$ , shift of emission maxima, lifetime) indicate thermo-reversible sol-gel transition of pluronics (P123, F127). Additionally, parameters  $I_{\text{neutral}}/I_{\text{anion}}$  and  $A_{\text{neutral}}/A_{\text{anion}}$  show sensitivity towards the micro-polarity of different pluronics. Moreover, with increasing temperature, the proton transfer rate has been found to decrease remarkably up to the sol-gel transition temperature, followed by a labeling effect. The rate of proton transfer depends on the availability of water molecules inside the pluronic micelles. Hence, a decrease in the proton transfer rate actually signifies expulsion of water molecules during sol-gel transition. Finally, from this study, 4-chloro-1-naphthol, a staining agent, emerges as a potent excited state proton transfer (ESPT) fluorescent molecular probe for studying the thermotropic sol-gel transition, thermo-reversible dehydration and micro-polarity of pluronics.

## Acknowledgements

I. S. thanks CSIR, New Delhi, India for her research fellowship and Prof. A. K. Mishra, Department of Chemistry, IIT Madras, for usage of the spectrofluorometer (Fluoromax 4, Horiba Jobin Yvon).

## References

- 1 A. Weller, *Prog. React. Kinet.*, 1961, **1**, 187.
- 2 T. Förster, *Elektrochemie*, 1950, **54**, 42.

- 3 A. K. Mishra, in "Understanding and Manipulating Excited State Processes", *Molecular and Supramolecular Photochemistry Series*, ed. V. Ramamurthy and K. S. Schanze, Marcel Dekker, Inc, New York, 2001, ch. 10, vol. 8, p. 577.
- 4 J. Waluk, *Conformational analysis of molecule in excited states*, Wiley-VCH, Weinheim, 2000.
- 5 A. Muller, in "Electron and proton transfer in chemistry and biology", *Studies in physical and theoretical chemistry*, ed. H. Ratajczak, W. Junge and E. Diemann, series 78, Elsevier science publishers B. V., Amsterdam, 1992.
- 6 M. Mouslmani and D. Patra, *RSC Adv.*, 2014, **4**, 8317.
- 7 C. Banerjee, S. Maiti, M. Mustafi, J. Kuchlyan, D. Banik, N. Kundu, D. Dhara and N. Sarkar, *Langmuir*, 2014, **30**, 10834.
- 8 S. Ghosh, J. Kuchlyan, D. Banik, N. Kundu, A. Roy, C. Banerjee and N. Sarkar, *J. Phys. Chem. B*, 2014, **118**, 11437.
- 9 A. P. Demchenko, K. C. Tang and P. T. Chou, *Chem. Soc. Rev.*, 2013, **42**, 1379.
- 10 D. Ghosh, A. K. Pradhan, S. Mondal, N. A. Begum and D. Mandal, *Phys. Chem. Chem. Phys.*, 2014, **16**, 8594.
- 11 V. S. Padalkar and S. Seki, *Chem. Soc. Rev.*, 2016, **45**, 169.
- 12 D. Sahoo and S. Chakravorti, *Photochem. Photobiol. Sci.*, 2010, **9**, 1094.
- 13 D. Mandal, S. K. Pal and K. Bhattacharyya, *J. Phys. Chem. A*, 1998, **102**, 9710.
- 14 P. Dutta, A. Halder, S. Mukherjee, P. Sen, S. Sen and K. Bhattacharyya, *Langmuir*, 2002, **18**, 7867.
- 15 J. Sujatha and A. K. Mishra, *J. Photochem. Photobiol., A*, 1997, **104**, 173.
- 16 M. Mohapatra and A. K. Mishra, *Langmuir*, 2011, **27**, 13461.
- 17 J. Sujatha and A. K. Mishra, *Langmuir*, 1998, **14**, 2256.
- 18 A. C. Kumar and A. K. Mishra, *Talanta*, 2007, **71**, 2003.
- 19 D. Sukul, S. K. Pal, D. Mandal, S. Sen and K. Bhattacharyya, *J. Phys. Chem. B*, 2000, **104**, 6128.
- 20 S. P. Webb, L. A. Phillips, S. W. Yeh, L. M. Tolbert and J. H. Clark, *J. Phys. Chem.*, 1986, **90**, 5154.
- 21 J. Swain and A. K. Mishra, *Phys. Chem. Chem. Phys.*, 2015, **17**, 16752.
- 22 N. Pappayee and A. K. Mishra, *Indian J. Chem.*, 2000, **39**, 964.
- 23 E. Fortin, P. Mailley, L. Lacroix and S. Szunerits, *Analyst*, 2006, **131**, 186.
- 24 Z. Wu, J. Wu, S. Wang, G. Shen and R. Yu, *Biosens. Bioelectron.*, 2006, **22**, 207.
- 25 T. U. Obi and C. K. Ojeh, *J. Clin. Microbiol.*, 1989, **27**, 2096.
- 26 R. M. Roop, D. Preston-Moore, T. Bagchi and G. G. Schurig, *J. Clin. Microbiol.*, 1987, **25**, 2090.
- 27 T. P. Lin, C. C. Liu, S. W. Chen and W. Y. Wang, *Plant Physiol.*, 1989, **91**, 1445.
- 28 H. Hudig and G. Drews, *J. Bacteriol.*, 1985, **162**, 897.
- 29 Z. Maskos and G. W. Winston, *J. Biol. Chem.*, 1994, **269**, 31579.
- 30 Y. V. Ilichev, A. B. Demyashkevich and M. G. Kuzmin, *J. Phys. Chem.*, 1991, **95**, 3438.
- 31 V. Balzani and L. de Cola, *Supramol. Chem.*, Springer Science & Business Media, 2012.
- 32 G. W. Robinson, P. S. Thistlewaite and J. Lee, *J. Phys. Chem.*, 1986, **90**, 4224.

- 33 P. Alexandridis and T. A. Hatton, *Colloids Surf., A*, 1995, **96**, 1.
- 34 K. S. Mali and G. B. Dutt, *J. Chem. Sci.*, 2007, **119**, 147.
- 35 R. Ganguly, V. K. Aswal, P. A. Hassan, I. K. Gopalakrishnan and S. K. Kulshreshtha, *J. Phys. Chem. B*, 2006, **110**, 9843.
- 36 I. Goldmints, F. K. von Gottberg, K. A. Smith and T. A. Hatton, *Langmuir*, 1997, **13**, 3659.
- 37 M. E. Mohanty, V. J. Rao and A. K. Mishra, *Spectrochim. Acta, Part A*, 2014, **121**, 330.
- 38 A. V. Kabanov, I. R. Nazarova, I. V. Astafieva, E. V. Batrakova, V. Y. Alakhov, A. A. Yaroslavov and V. A. Kabanov, *Macromolecules*, 1995, **28**, 2303.
- 39 K. T. Oh, T. K. Bronich and A. V. Kabanov, *J. Controlled Release*, 2004, **94**, 411.
- 40 E. V. Batrakova and A. V. Kabanov, *J. Controlled Release*, 2008, **130**, 98.
- 41 I. Sarkar, H. S. P. Rao, A. Desai and A. K. Mishra, *RSC Adv.*, 2015, **5**, 97279.
- 42 Y. Kadam, U. Yerramilli and A. Bahadur, *Colloids Surf., B*, 2009, **72**, 141.
- 43 K. Nakashima and P. Bahadur, *Adv. Colloid Interface Sci.*, 2006, **123–126**, 75.
- 44 S. George, M. Kumbhakar, P. K. Singh, R. Ganguly, S. Nath and H. Pal, *J. Phys. Chem. B*, 2009, **113**, 5117.
- 45 C. Chaibundit, N. M. P. S. Ricardo, F. de M. L. L. Costa, S. G. Yeates and C. Booth, *Langmuir*, 2007, **23**, 9229.
- 46 J. R. Lakowicz, *Principles of Fluorescence Spectroscopy*, Springer Publishers, New York, 3rd edn, 2006.
- 47 G. Wanka, H. Hoffmann and W. Ulbricht, *Macromolecules*, 1994, **27**, 4145.
- 48 J. J. Escobar-Chavez, M. Lopez-Cervantes, A. Naik, Y. N. Kalia, D. Quintanar-Guerrero and A. Ganem-Quintanar, *J. Pharm. Pharm. Sci.*, 2006, **9**, 339.
- 49 H. S. P. Rao, A. Desai, I. Sarkar, M. Mohapatra and A. K. Mishra, *Phys. Chem. Chem. Phys.*, 2014, **16**, 1247.
- 50 I. Sarkar, A. Hemamalini, T. M. Das and A. K. Mishra, *RSC Adv.*, 2016, **6**, 27933.
- 51 P. Sen, S. Ghosh, K. Sahu, S. K. Mondal, D. Roy and K. Bhattacharyya, *J. Chem. Phys.*, 2006, **124**, 204905.
- 52 K. Bhattacharyya, *Acc. Chem. Res.*, 2003, **36**, 95.